Overlapped Complex-Modulated Transmultiplexer Filters With Simplified Design and Superior Stopbands

Shahriar Mirabbasi, *Member, IEEE,* and Ken Martin, *Fellow, IEEE*

***Abstract*—A simple method for the design of the finite-impulse-response prototype filter for maximally decimated overlapped complex-modulated transmultiplexers with near perfect reconstruction property is presented. The procedure is unified for all values of overlap factor and leads to a prototype filter with excellent frequency selectivity and fast sidelobe fall-off rate. The high stopband attenuation and fast sidelobe fall-off rate, which is justified analytically, make the proposed filters suitable candidates for high-speed data communication applications employing multicarrier modulation.**

***Index Terms*—Complex modulation, filter banks, multicarrier systems, multirate, near-perfect reconstruction, overlapped filter banks, pseudo-quadrature mirror filter (QMF), transmultiplexes.**

I. Introduction

MULTICARRIER modulation is an efficient technique for transmitting information, especially broad-band data, over wireline and wireless channels. This modulation scheme can be described in the context of filter-bank-based transmultiplexers (TMUXs) [1]–[5]. In efficient contemporary implementations of multicarrier modulation, known as discrete multitone modulation (DMT) or orthogonal frequency-division multiplexing (OFDM), modulation and demodulation are performed digitally using the inverse discrete Fourier transform (IDFT) and the discrete Fourier transform (DFT). However, given a practical communication channel, the significant spectral overlap between signaling filters in a DFT-based filter bank (sidelobes on the order of -13 dB) results in performance degradation of the system [4], [6], [7]. For example, a narrow-band interference in a frequency band could degrade several subchannels and make them unusable even when the interferer center frequency is widely separated from that of those subchannels.

To alleviate the problems associated with the poor frequency selectivity of subchannel filters in DFT-based multitone systems, alternative filter-bank-based techniques, such as the overlapped DMT, or the discrete wavelet multitone (DWMT) are proposed [4], [6], [7]. These filter banks use finite-impulse response (FIR) filters of a length greater than that of rectangular filters in DFT-based systems and result in better subchannel spectral containment, without sacrificing the Nyquist properties of the set of subchannel waveforms. Better stopband attenuation and subchannelization result in both lower levels of interchannel interference (ICI) and greater robustness to narrow-band interference [4], [7]. For an M-channel system, the length of the subchannel filters is typically gM with $g > 1$ (as opposed to $g = 1$ in conventional DMT systems). Thus, the pulse waveforms for different symbol blocks overlap in time, and hence g is called the overlap-factor.

In realizing these alternative filter-bank-based TMUXs, complex-modulated or cosine-modulated filter banks are used, depending on the application (i.e., whether the baseband signals are complex or real). In these types of filter banks, synthesis and analysis filters are typically derived from a prototype filter; therefore, the number of parameters to be optimized is small compared to a general filter bank. Moreover, efficient implementation techniques exist for both complex- or cosine-modulated filter banks [4], [8].

In this paper, we consider the case of a complex-modulated TMUX, in which the subchannel filters have possibly complex coefficients. Historically, the first modulated filter banks that were known to offer an efficient implementation were the complex-modulated filter banks. They are also called DFT filter banks since they can be realized efficiently using the DFT transform [8], [9]. To achieve filters with real coefficients, standard methods can be employed, such as combining two filters that have complex conjugate coefficients in the synthesis (or analysis) bank. These methods are similar to techniques used in cosine-modulated filter banks [8], [11].

Also, we focus on a TMUX system with near-perfect-reconstruction (NPR) property (assuming an ideal channel). As mentioned in [1] and [6], it is often judicious to relax the perfect reconstruction (PR) condition by allowing small amplitude and crosstalk (aliasing) distortion, and at the same time achieving better stopband performance (increased frequency selectivity) of subchannel filters. It is worth mentioning that, due to the duality between maximally-decimated filter banks [also known as quadrature mirror filter (QMF) banks] and transmultiplexer systems [8], [11], [13], the results here can also be applied to the design of a prototype filter for complex-modulated NPR QMF banks (pseudo-QMF banks).

The most significant features of the proposed approach include: 1) a simple and exact prototype filter design procedure given a few tabulated parameters that is applicable to different

Manuscript received April 23, 2002; revised April 8, 2003. This work was supported in part by Natural Sciences and Engineering Research Council of Canada (NSERC) Grant.

S. Mirabbasi is with the Department of Electrical and Computer Engineering, University of British Columbia, Vancouver, BC V6T 1Z4, Canada (e-mail: shahriar@ece.ubc.ca).

K. Martin is with the Department of Electrical and Computer Engineering, University of Toronto, Toronto, ON M5G 1G6, Canada.

Digital Object Identifier 10.1109/TCSII.2003.813592

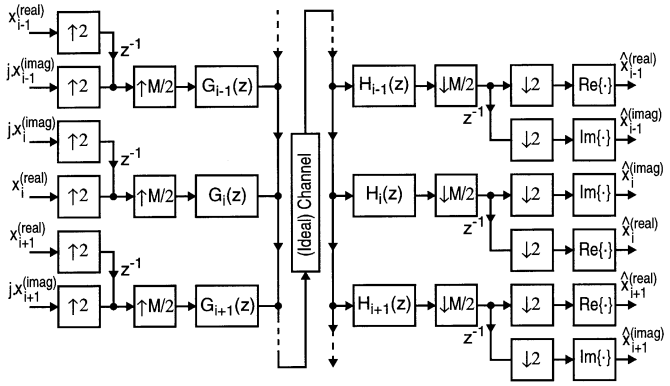

Fig. 1. Modified DFT transmultiplexer.

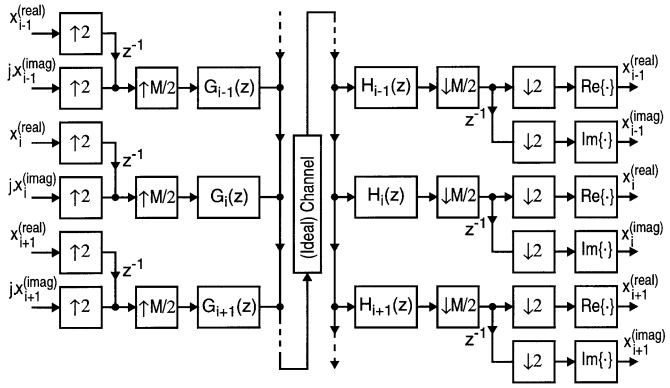

Fig. 2. TMUX system considered in this work.

filter orders and overlap factors (for overlap factors of 3 to 8 all these parameters are tabulated in Table I) and 2) superior stopband fall-off rates and attenuation for increasing frequency differences from individual channel passbands. The latter feature is desirable in data-communication applications having interferers.

The NPR TMUX system that we consider is a variation of the modified DFT (MDFT) TMUX [10], [11], which will be briefly reviewed in Section II. The design procedure for the prototype filter with good stopband fall-off performance is discussed in Section III, where the fast fall-off rate of the designed filter spectrum is justified analytically. Comparison with other design approaches is included in Section IV.

II. MDFT TMUXs

An MDFT TMUX [10]–[12] is shown in Fig. 1, in which the number of channels M is assumed to be even. In this system, all the filters in the filter bank are derived by complex modulation from an FIR baseband prototype filter with frequency response $P(e^{j\omega})$ (where $j = \sqrt{-1}$)

$$G_i(e^{j\omega}) = M \cdot P\left(e^{j(\omega - \frac{2\pi i}{M})}\right), \quad i = 0, 1, \ldots, M-1 \quad (1)$$

$$H_i(e^{j\omega}) = P\left(e^{j(\omega - \frac{2\pi i}{M})}\right), \quad i = 0, 1, \ldots, M-1. \quad (2)$$

It is called a modified DFT TMUX because of the following additional modifications to the DFT filter bank [11]. The real and imaginary parts of the input and output signals to the TMUX are staggered by the offset of $M/2$ and the assignment of real and imaginary parts to the inputs and outputs of each channel alternates from channel to channel, as illustrated in Fig. 1.

It can be shown [9]–[11] that the overall MDFT TMUX system has a structurally inherent crosstalk (alias) cancellation, i.e., the crosstalk between adjacent channels is cancelled. (In fact, in addition to crosstalk between the adjacent channels, the crosstalk between any two channels where the difference between their indices is an odd number, e.g., second and fifth channels, is also cancelled.) The remaining crosstalk between nonadjacent channels can be kept arbitrarily small by appropriate design of the prototype filter (and its stopband attenuation). A prototype filter with good spectral containment, in which the stopband attenuation increases for greater frequency differences from its passband edge, would minimize the crosstalk. The design of a class of such a prototype filter is the subject of this paper.

The TMUX system considered in this paper has an architecture that is slightly different from that of the standard MDFT TMUX. It is similar to the TMUX system in [6], in which the synthesis and analysis filters of the TMUX are constructed from a prototype filter as follows:

$$G_i(e^{j\omega}) = j^i \cdot P\left(e^{j(\omega - \frac{2\pi i}{M})}\right), \quad i = 0, 1, \ldots, M-1 \quad (3)$$

$$h_i(n) = g_i^*(N-n), \quad i = 0, 1, \ldots, M-1. \quad (4)$$

In (4), N is the order of the prototype filter, and $*$ represents complex conjugation. The frequency-domain equivalent of (4) is

$$H_i(e^{j\omega}) = e^{-jN\omega} G_i^*(e^{j\omega}). \quad (5)$$

The inclusion of the factor j^i in the synthesis (transmit) filters does not change the magnitude of their frequency response; it is equivalent to and in lieu of alternating the assignment of real and imaginary parts of the inputs and outputs in the MDFT TMUX. The block diagram of this variation of the standard MDFT TMUX is shown in Fig. 2. It can be shown (similar to [9], [12]) that the TMUX in Fig. 2 has structurally-inherent crosstalk cancellation property. This is discussed in more detail in Appendix A.

III. Prototype Design

In this work, we assume that the prototype filter belongs to a class of real low-pass filters with the impulse response of the following general form:

$$p(n) = \begin{cases} \frac{1}{N}\left(k_0 + 2\sum_{l=1}^{g-1} k_l \cos\left(\frac{2\pi l n}{N}\right)\right), & 0 \le n \le N \\ 0, & \text{otherwise} \end{cases} \quad (6)$$

where $N = gM$, and $k_l s (0 \le l < g)$ are real coefficients. Here the overlap factor g is a positive integer and M, the number of channels in the TMUX system, is an even number. Note that the prototype filter introduced in [6] has the same general form as in (6). Also notice that the well-known Hamming, Hanning, and Blackman windows are special cases of this prototype low-pass filter [14], i.e., with $k_0 = 0.5$ and $2k_1 = -0.5$ ($k_0 = 0.54$ and $2k_1 = -0.46$), $p(n)$ represents the Hanning (Hamming)

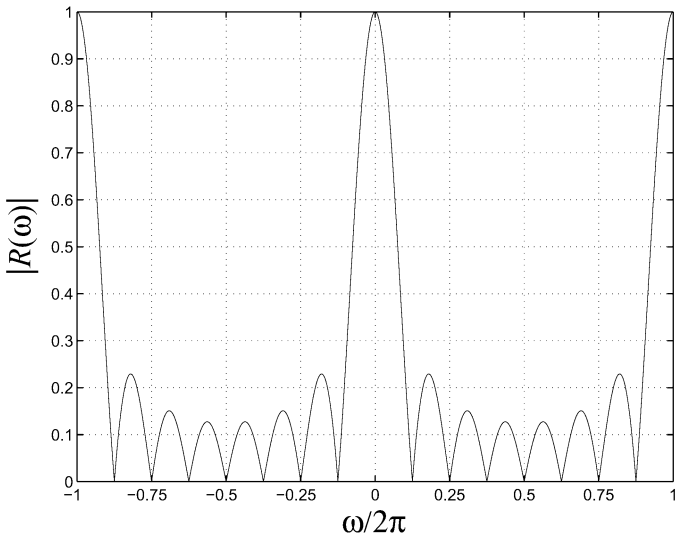

Fig. 3. Plot of $|R(\omega)|$ for $N = 8$ (the horizontal axis is normalized to 2π).

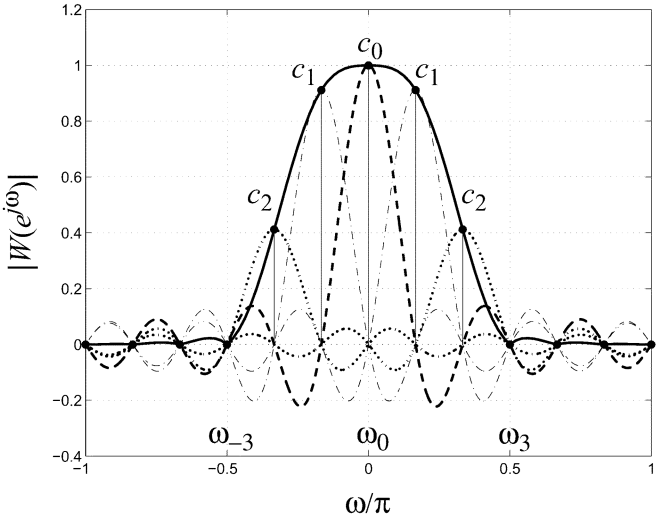

Fig. 4. Example frequency response $W(e^{j\omega})$ for $g = 3$ and $M = 4 (N = 12)$.

window, and, with $k_0 = 0.42$, $2k_1 = -0.50$, and $2k_2 = -0.08$, $p(n)$ realizes the Blackman window.

We will now discuss the requirements for the coefficients $k_l (0 \le l < g)$, which in addition to providing a good stopband performance of the channel filters, result in a near-perfect reconstruction property of the TMUX.

If we temporarily ignore the causality requirements, then a low-pass filter having an impulse response of the form

$$w(n) = \begin{cases} \frac{1}{N}\left(c_0 + 2\sum_{l=1}^{g-1} c_l \cos\left(\frac{2\pi l n}{N}\right)\right), & -\frac{N}{2} \le n \le \frac{N}{2} \\ 0, & \text{otherwise} \end{cases} \tag{7}$$

with $N = gM$, has even-symmetry (i.e., $w(n) = w(-n)$) and hence is a linear-phase filter. As mentioned earlier, filters of this general form have already been used in the context of window design to achieve a good stopband performance as well as a fast sidelobe fall-off rate [14]–[17].

It can be shown [21] that the Fourier transform of a low-pass filter of the form (7) is

$$W(e^{j\omega}) = c_0 R(\omega) + \sum_{l=1}^{g-1} c_l \left(R\left(\omega - \frac{2\pi l}{N}\right) + R\left(\omega + \frac{2\pi l}{N}\right)\right) \tag{8}$$

where $R(\omega) = (e^{j(\omega/2)}/N) \cdot ((\sin(N\omega/2))/(\sin(\omega/2)))$ is the Fourier transform of an N-point rectangular window $r(n)$, i.e.,

$$r(n) = \begin{cases} 1, & -\frac{N}{2} \le n < \frac{N}{2} \\ 0, & \text{otherwise.} \end{cases}$$

For an even number N, $R(\omega)$ is a periodic function with period 2π ($|R(\omega)|$ is 2π-periodic for any integer number N). A plot of $|R(\omega)|$ for the case of $N = 8$ is shown in Fig. 3.

Note that from (8) we can see that $W(e^{j\omega})$ is a linear combination of frequency-shifted copies of $R(\omega)$, with frequency shifts being an integer multiple of $2\pi/N$.

Defining uniformly-spaced frequencies around the unit circle (l is an integer number)

$$\omega_l = \frac{2\pi l}{N} \tag{9}$$

we have

$$R(\omega_l) = \begin{cases} 1, & l = 0, \pm N, \pm 2N, \ldots \\ 0, & \text{otherwise.} \end{cases} \tag{10}$$

Using (9) and (10) in (8) results in

$$W(e^{j\omega_l}) = \begin{cases} c_l, & l = 0, \pm 1, \pm 2, \ldots, \pm(g-1) \\ 0, & l = \pm g, \pm(g+1), \ldots, \pm\frac{N}{2}. \end{cases} \tag{11}$$

Since $W(e^{j\omega})$ is 2π-periodic, only the l s for which $-\pi \le \omega_l \le \pi$ are considered in (11). It can be seen that $c_l s$ are the sample values of $W(e^{j\omega})$ sampled at corresponding ω_l's (in fact our discussion is similar to that of the frequency sampling technique for designing FIR filters [21]). Hence, $W(e^{j\omega})$ can be thought of as the interpolation of sample values $W(e^{j\omega_l})$, with interpolation functions being copies of $R(\omega)$ displaced by integer multiples of $2\pi/N$. This is illustrated graphically in Fig. 4 for $g = 3$ and $M = 4 (N = 12)$. As can be seen in this figure, with a proper choice of $c_l s$, the shifted scaled copies $R(\omega \pm (2\pi l)/N)$ tend to cancel the sidelobe ripples from $R(\omega)$, thereby reducing considerably the overall sidelobe level (at the expense of widening the mainlobe width of the frequency response).

From (11), it can be observed that the mainlobe width of the filter is $\omega_g = 2\pi g/N = 2\pi/M$ (the first sample frequency at which $W(e^{j\omega})$ is zero). For instance, the mainlobe width of the filter in Fig. 4 is $\omega_3 = 2\pi \cdot 3/12 = 2\pi/4$. As will be discussed later, with a proper choice of coefficient $c_l s$, the -3 dB bandwidth of this filter would be π/M, which is the desirable choice for M-channel TMUX applications [6], [8], [11].

Note that $c_l s (0 \le l < g)$ are the passband and transition-band sample values of the low-pass frequency response $W(e^{j\omega})$. In order for the prototype filter to have a reasonably smooth transition region, we add two additional constraints

on the coefficients. First, we require the coefficients c_l's $(0 \leq l < g)$ to all be positive. In fact, it suffices that all the coefficients be of the same sign, i.e., all negative or all positive. If two of the coefficients, for example c_l and c_{l+1} have different signs, then $W(e^{j\omega})$ would have a zero crossing between frequencies ω_l and ω_{l+1}. This is undesirable, because ω_l and ω_{l+1} are either in the passband or the transition-band of the filter, where we do not want any zero crossing to happen.

The second constraint on the coefficients is that they should be monotonically decreasing in absolute value. This should be clear, since, according to (11), the coefficients $c_l s$ are the magnitudes of the $W(e^{j\omega})$ sampled at corresponding frequencies ω_l in the pass- and transition-bands of the filter. Given the low-pass nature of the filter, it is required that the magnitude of the coefficients be in decreasing order.

Assuming that the coefficients are all positive, the two constraints stated above translate into

$$c_0 > c_1 > \ldots > c_{g-2} > c_{g-1} > 0. \tag{12}$$

Without loss of generality, we assume that c_0, which is the magnitude of the frequency response $W(e^{j\omega})$ at $\omega = 0$, is normalized to one, i.e., $c_0 = 1$. We will also justify this assumption later on, when we discuss the requirements for the prototype filter, in order for the overall TMUX to have a near perfect reconstruction property.

We construct our prototype filter from a causal version of the FIR low-pass filter of (7), that is, by shifting the time index by $N/2$ samples, i.e.,

$$p(n) = w\left(n - \frac{N}{2}\right) \tag{13}$$

where

$$w\left(n-\frac{N}{2}\right) = \begin{cases} \frac{1}{N}\left(c_0 + 2\sum_{l=1}^{g-1} c_l \right. \\ \quad \left. \times \cos\left(\frac{2\pi l n}{N} - \pi l\right)\right), & 0 \leq n \leq N \\ 0, \quad \text{otherwise.} \end{cases} \tag{14}$$

Thus

$$p(n) = \begin{cases} \frac{1}{N}\left(c_0 + 2\sum_{l=1}^{g-1} (-1)^l c_l \right. \\ \quad \left. \times \cos\left(\frac{2\pi l n}{N}\right)\right), & 0 \leq n \leq N \\ 0, \quad \text{otherwise.} \end{cases} \tag{15}$$

Comparing the right-hand sides of (6) and (15) we have

$$k_l = (-1)^l c_l, \qquad 0 \leq l < g. \tag{16}$$

Since $c_l > 0$ for $0 \leq l < g$, (16) indicates that the adjacent coefficients of the prototype filter should have alternating signs, with k_0 being positive. This fact was heuristically justified in [6].

Next, we discuss the conditions on k_l's (for $0 \leq l < g$) required for $p(n)$ to have a fast fall-off rate of its sidelobes. For continuous-time functions, it is known that the smoother a function is, as measured by the number of continuous derivatives it possesses, the more compact is its Fourier transform; that is, the faster its transform dies away with increasing frequency. In fact, if a continuous-time function and its first k derivatives are continuous, its Fourier transform dies away at least as rapidly as $|\Omega|^{-(k+2)}$ for large Ω(Ω being the frequency in rad/s) [18], [19].

Although this theorem has also been used for the case of discrete-time windows [14], special care should be given to applying the theorem to discrete-time functions. The subtle point is in the interpretation of continuity and the existence of derivatives for discrete-time functions. However, if a discrete-time function is a sampled version of a smooth, continuous-time function with a high enough sampling rate, then, assuming the Fourier transform of the underlying continuous-time function dies away at least as rapidly as $|\Omega|^{-k}$, the rate of fall-off of the sidelobes of the corresponding sampled (discrete-time) function would be approximately $|\omega|^{-k}$ ($\omega = \Omega T$ is the scaled discrete-time frequency, and T is the sampling period).

In our case, the prototype filter is a sampled version of the following continuous-time function:

$$p_c(t) = \begin{cases} \frac{1}{N}\left(k_0 + 2\sum_{l=1}^{g-1} k_l \cos(l\Omega_N t)\right), & 0 \leq t \leq NT \\ 0, \quad \text{otherwise} \end{cases} \tag{17}$$

where $\Omega_N = 2\pi/(NT)$ and T is the sampling period.

With a proper choice of coefficients k_l (for $0 \leq l < g - 1$), the Fourier transform of $p_c(t)$ has a -3-dB bandwidth of $\Omega = \pi/(MT)$, mainlobe width of $\Omega = 2\pi/(MT)$ with $M = N/g$, and a fast fall-off rate [6]. Hence, by sampling $p_c(t)$ with the sampling period of T, we are in fact oversampling $p_c(t)$ by roughly a factor of $M/2$. As a result, the effect of aliasing in the discrete-time Fourier transform of $p(n) = p_c(nT)$ becomes less significant, especially as M (and thus, the oversampling factor) becomes larger. Consequently, if the Fourier transform of $p_c(t)$ falls off at the rate of $|\Omega|^{-k}$, then the fall-off rate of the discrete Fourier transform of $p(n)$ would be $|\omega|^{-k}$.

The cosine functions in the summation of (17) are continuous, and so are all their derivatives, except perhaps at the boundary points: $t = 0$ and $t = NT$. Hence, the only points that need to be considered for the purpose of smoothness of this function are the boundary points. Due to the symmetry of $p_c(t)$ with respect to $t = NT/2$, i.e., $p_c(t) = p_c(t - NT)$ for $0 \leq t \leq NT$, it suffices to check for the continuity of the function and its derivatives only at the boundary point $t = 0$.

Note that, because of the special form of $p_c(t)$, its odd order derivatives are already continuous at the boundary points. This is because

$$p_c^{(r)}(t) = \begin{cases} \frac{2}{N}\sum_{l=1}^{g-1} (-1)^{\alpha} (l\Omega_N)^r k_l \sin(l\Omega_N t), & 0 \leq t \leq NT \\ 0, \quad \text{otherwise} \end{cases} \tag{18}$$

where $p_c^{(r)}(t)$ is the rth-order derivative of $p_c(t)$ with respect to t, and r is an odd positive integer. The integer number α is a function of r, and its value is immaterial for the purpose of our discussion. As can be seen from (18), at the boundary point $t = 0$, any odd-order derivative of $p_c(t)$ is continuous, and $p_c^{(r)}(t) = 0$.

Thus, for a positive and even integer number q, if the qth order derivative of $p_c(t)$ at boundary point $t = 0$ is continuous, then the Fourier transform of $p_c(t)$ falls off at the rate of at least $|\Omega|^{-(q+3)}$. This is due to the fact that the $(q+1)$th order derivative would be continuous as well (since $q+1$ would be an

odd number). As explained earlier, this implies that the fall-off rate of the discrete Fourier transform of $p(n)$ would be approximately $|\omega|^{-(q+3)}$.

Now let us discuss the conditions required for continuity of $p_c(t)$ and its even-order derivatives. For $p_c(t)$ to be continuous at $t = 0$ (or, equivalently, its zeroth-order derivative to be continuous), we need $p_c(0) = 0$. Considering (17), this requires

$$k_0 + 2\sum_{l=1}^{g-1} k_l = 0. \tag{19}$$

This requirement was also heuristically justified in [6]. Note that if (19) is satisfied, then the sidelobes of the discrete Fourier transform of $p(n)$ would have the approximate fall-off rate of $|\omega|^{-3}$. This fall-off rate is significantly faster than the fall-off rate of filters in standard DFT based TMUXs, which, due to the use of rectangular windowing, have a fall-off rate of $|\omega|^{-1}$.

For an even integer q (with $q \geq 2$), the qth order derivative of $p_c(t)$ has the form

$$p_c^{(q)}(t) = \begin{cases} \frac{2}{N}\sum_{l=1}^{g-1}(-1)^{\beta}(l\Omega_N)^q k_l \cos(l\Omega_N t), & 0 \leq t \leq NT \\ 0, & \text{otherwise} \end{cases} \tag{20}$$

where the integer number β is a function of q, and its value is inconsequential for the purpose of our discussion. In order for $p_c^{(q)}(t)$ to be continuous at $t = 0$, we should have $p_c^{(q)}(0) = 0$. This requires

$$\frac{2}{N}\sum_{l=1}^{g-1}(l\Omega_N)^q k_l = 0, \qquad q \geq 2 \tag{21}$$

which can be simplified to

$$\sum_{l=1}^{g-1} l^q k_l = 0, \qquad q \geq 2. \tag{22}$$

As discussed earlier, if (22) holds for even-integer number q, then the fall-off rate of $P(e^{j\omega})$ would be approximately $|\omega|^{-(q+3)}$.

So far, we have focused on the conditions required for the coefficients k_l, such that the spectrum of the prototype filter $p(n)$ has a fast fall-off rate (good stopband performance). We will now discuss the required properties of the coefficients k_l, in order for the complex-modulated TMUX shown in Fig. 3 to have a near-perfect-reconstruction property.

As mentioned before, the MDFT TMUX of Fig. 2 has structurally-inherent crosstalk cancellation; thereby the crosstalk between any two channels with an odd-numbered difference between their indices (including any two adjacent channels) is cancelled. Furthermore, assuming that the channel filters have a high stopband attenuation and a fast sidelobe fall-off rate, the remaining crosstalk between nonadjacent channels would be negligible. Then, as outlined in [3], [9], [11], [12], the overall TMUX system has a (near) perfect-reconstruction property if for some $c > 0$ the following condition (approximately) holds:

$$\left|\sum_{i=0}^{M-1} G_i(e^{j\omega})H_i(e^{j\omega})\right| = c. \tag{23}$$

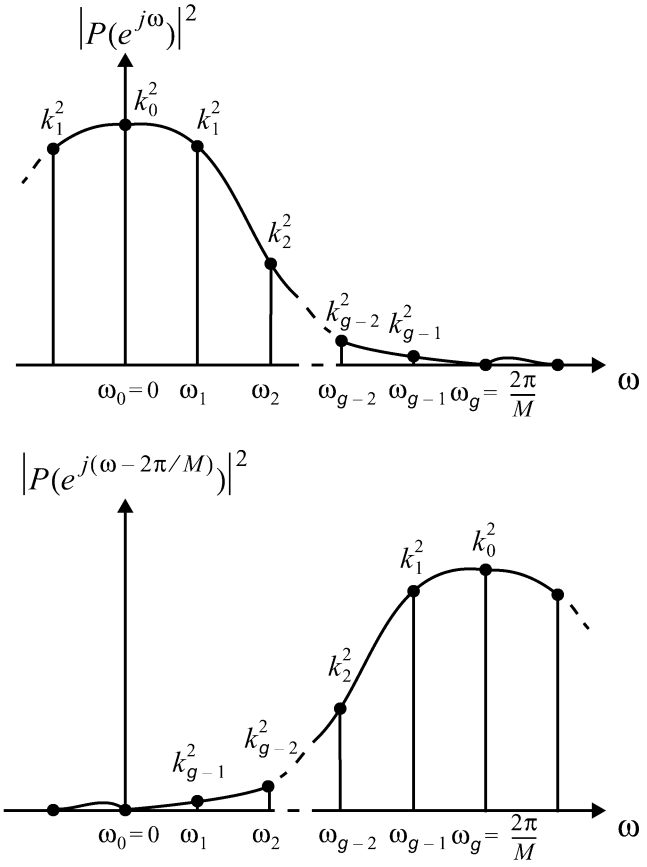

Fig. 5. Plots of $|P(e^{j\omega})|^2$ and $|P(e^{j(\omega-2\pi/M)})|^2$.

That is, $\sum_i G_i(e^{j\omega})H_i(e^{j\omega})$ should be (approximately) an all-pass filter. Using (5) in (23), we have

$$\left|\sum_{i=0}^{M-1} G_i(e^{j\omega})e^{-jN\omega}G_i^*(e^{j\omega})\right| = \sum_{i=0}^{M-1}\left|G_i(e^{j\omega})\right|^2 = c. \tag{24}$$

Substituting (3) in (24), leads to

$$\sum_{i=0}^{M-1}\left|P\left(e^{j(\omega-\frac{2\pi i}{M})}\right)\right|^2 = c. \tag{25}$$

In other words, in order to have a (near) PR complex-modulated TMUX, the prototype filter should have the (approximate) power-complementary property [3], [6], [8], [11]. Without loss of generality, we can assume that $c = 1$. Due to the special form of the prototype filter, as mentioned in [6], if the equality in (25) holds for the set of discrete sample frequencies of (9) (i.e., ω_l's), then it will be approximately satisfied for any value of ω. We will now examine the requirements for coefficient $k_l s$ of the prototype filter, in order to satisfy (25) for $c = 1$ at discrete frequencies $\omega_l = (2\pi l)/N$

From (11), (13), and (16), we can write

$$\left|P(e^{j\omega_l})\right|^2 = \begin{cases} k_l^2, & l = 0, \pm 1, \pm 2, \ldots, \pm(g-1) \\ 0, & l = \pm g, \pm(g+1), \ldots, \pm\frac{N}{2}. \end{cases} \tag{26}$$

Again, since $|P(e^{j\omega})|$ is 2π-periodic, only the ls for which $-\pi \leq \omega_l \leq \pi$ are considered in (26). Note that among these

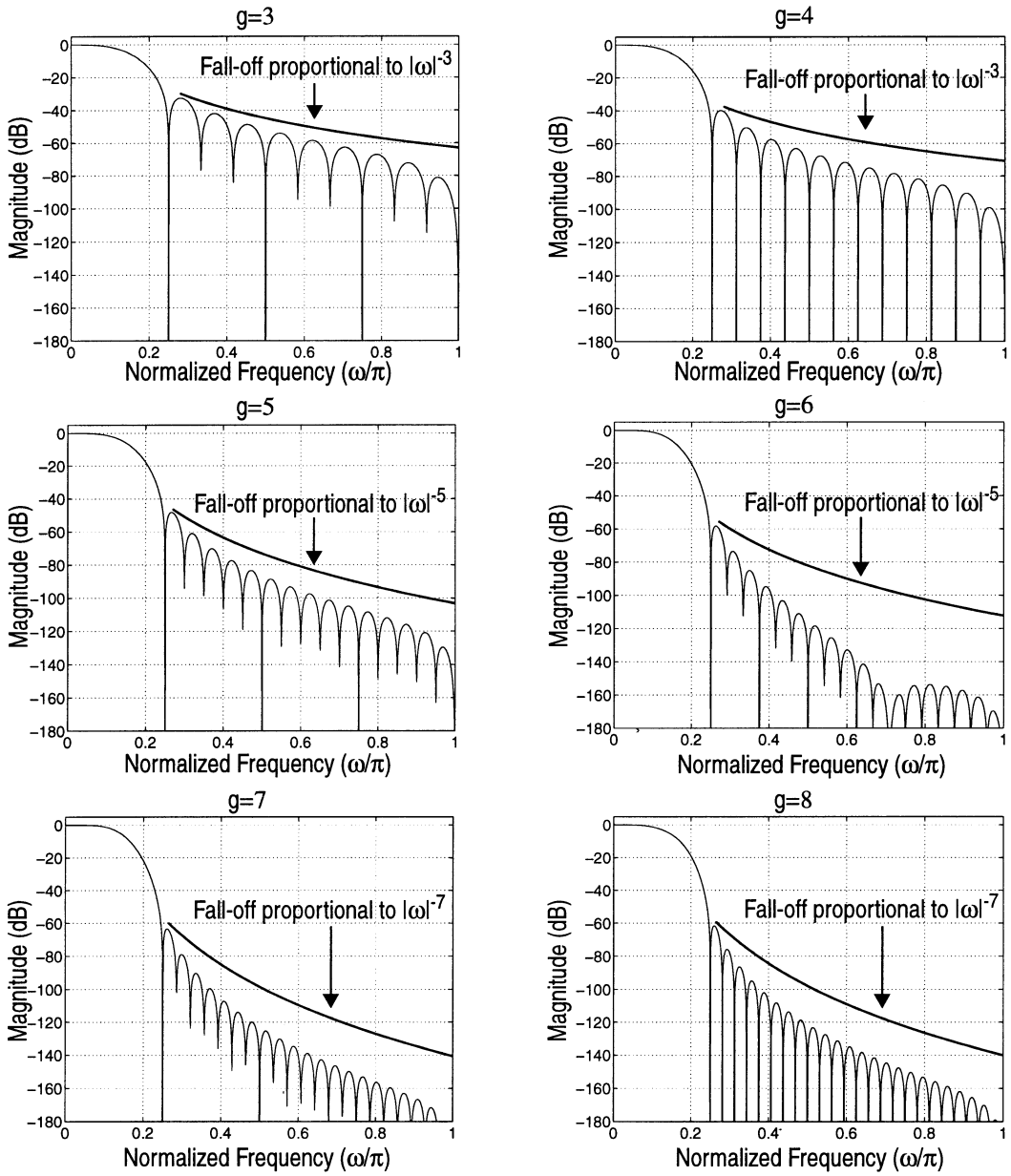

Fig. 6. Magnitude frequency response of the prototype filter for different values of the overlap factor g $(3 \leq g \leq 8)$.

values of l, $|P(e^{j\omega_l})|$ is nonzero for $|l| < g$, or, equivalently, $|\omega_l| < 2\pi/M$. In addition, because of the symmetry of the shifted copies of $|P(e^{j\omega})|$, i.e., $|P(e^{j(\omega-2\pi m/M)})|$, with respect to their center frequencies $((2\pi m)/M)$, it suffices to satisfy (25) at sample frequencies $\omega_l = (2\pi l)/N$ for $l = 0, 1, \ldots, g-1$. For this set of frequencies, the only nonzero magnitude frequency response samples on the left-hand side summation in (25) belong to $|P(e^{j\omega})|^2$ and $|P(e^{j(\omega-2\pi/M)})|^2$. These square magnitude frequency responses are illustrated in Fig. 5.

It can be seen from the Fig. 5 that in order to have the summation on the left-hand side of (25) be equal to unity at discrete frequencies ω_l's, we should have

$$\begin{cases} k_0 = 1 \\ k_l^2 + k_{g-l}^2 = 1, \quad l = 1, 2, \ldots \lfloor \frac{g}{2} \rfloor \end{cases} \tag{27}$$

where $\lfloor x \rfloor$ represents the largest integer that is less than or equal to x.

Note that in (27), k_0 is chosen to be 1, because, as explained earlier, we want k_0 to be positive. (From the original equation $k_0^2 = 1$, we have picked the positive solution). If coefficients k_l are chosen such that equations in (27) hold, then the -3-dB frequency of the prototype filter would be (approximately) π/M, when g is (odd) even. For the case of even g, the second equation in (27) for $l = g/2$ leads to $k_{g/2}^2 = 1/2$. Since $k_{g/2}^2$ is the magnitude square of $P(e^{j\omega})$ at frequency $\omega_{g/2} = \pi/M$, therefore the -3-dB frequency of the prototype filter is π/M.

Given the overlap-factor g, in order to realize the prototype filter, we need to find the g coefficients k_l's (for $0 \leq l \leq g$). In general, we need a system of g (independent) equations to solve for g coefficients k_l. Equations (19) and (27) account for $\lfloor g/2 \rfloor + 2$ equations ($g \geq 3$, to be able to construct a system of

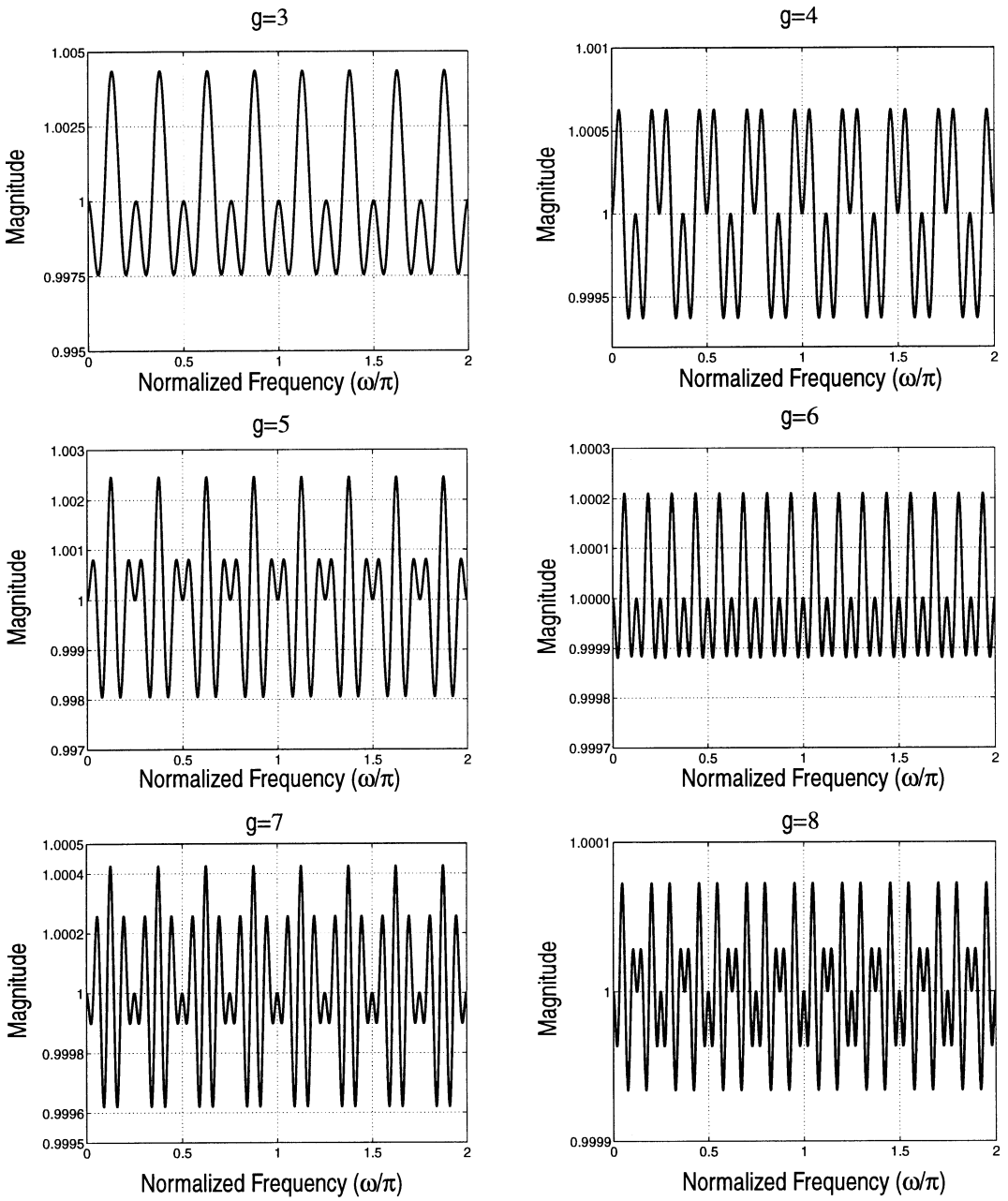

Fig. 7. Normalized magnitude of the linear distortion function [i.e., left-hand side of (23)] for an 8-channel TMUX constructed with a prototype filter for different values of the overlap factor g $(3 \leq g \leq 8)$.

equations with equal number of equations as that of unknowns). Equation (22) can be used to construct the remaining equations necessary to have a system of g equations. This system of equations contains quadratic equations [because of (27)], and, in general, it might have more than one set of solutions. An acceptable solution should satisfy the constraints that the adjacent coefficients of the prototype filter should have alternating signs starting with $k_0 = 1$ [due to (27)] and that the coefficients should have monotonically decreasing magnitudes. The values of example prototype filter coefficients for $3 \leq g \leq 8$ are tabulated in Table I. The magnitude frequency responses of these prototype filters for $3 \leq g \leq 8$ are depicted in Fig. 6.

Note that in Table I, the coefficient values of the prototype filter for $g > 4$ are different from those reported in [6]. Also, note that the proposed procedure for finding the coefficients is unified for any value of g, and is based on solving a system of g equations g unknowns. This is a further simplification compared to the method of [6], which for $g > 4$ is based on an iterative optimization procedure.

The minimum stopband attenuation (MSA) and the approximate rate of fall-off (ARF) of the sidelobes of $P(e^{j\omega})$ for different values of g are also given in Table I. The MSA was found to be only a function of the overlap factor g and independent of the filter order. The ARF can be determined based on the number of equations that are generated using (19) and (22) to find the coefficient values. For example, for $g = 5$, (27) and (19) provide us with four equations and the last equation is obtained from (22) using $q = 2$. This implies that the approximate fall-off rate of $P(e^{j\omega})$ is $|\omega|^{-5}$. As it can be seen from the magnitude frequency responses shown in Fig. 6, the fall-off rate of

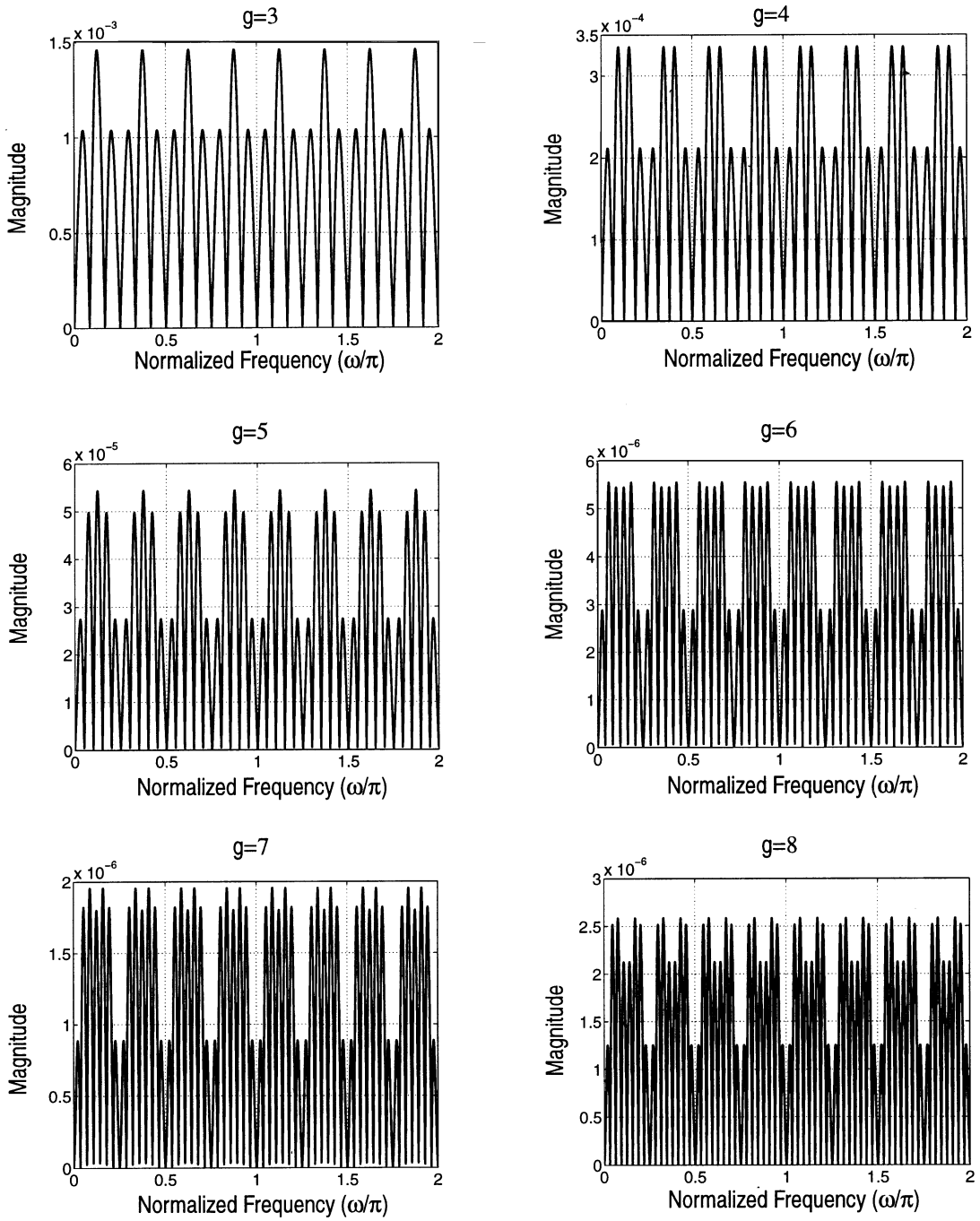

Fig. 8. Magnitude of the crosstalk distortion function of (A22) for an 8-channel TMUX constructed with a prototype filter for different values of the overlap factor g $(3 \leq g \leq 8)$.

the sidelobes of the prototype filter for different values of g is actually faster than the tabulated ARF in Table I.

Also listed in Table I are the signal-to-noise ratios (SNRs) of an 8-channel MDFT TMUX with the proposed prototype filter for different values of g. In calculating SNR, the only noise considered is reconstruction error, i.e., interchannel interference and errors due to crosstalk (aliasing) at the TMUX output. The inputs to the TMUX are taken from a sequence of random complex numbers, where real and imaginary parts are uniformly distributed between -1 and 1. As can be seen, the distortion due to reconstruction error is very small and negligible in most practical multicarrier applications [1], [6] and decreases as g increases.

To further illustrate the near-perfect-reconstruction property of the different TMUXs constructed using the prototype filters of Table I, Figs. 7, and 8 show the plots of the normalized magnitude of the linear distortion function [8], [9], (i.e., left-hand side of (23) and the crosstalk distortion measure of (A22).

IV. Comparison

In this section, we compare the performance of an MDFT TMUX based on the proposed prototype filter, with that of MDFT TMUXs based on other prototype filters. First, we consider the prototype filter design approach introduced in [22].

TABLE I
COEFFICIENTS OF THE PROTOTYPE FILTER FOR DIFFERENT VALUES OF G, ALONG WITH THE MINIMUM STOP-BAND ATTENUATION (MSA) AND APPROXIMATE RATE OF FALL-OFF (ARF) OF THE SIDELOBES OF $P(e^{j\omega})$ AND SNR OF AN 8-CHANNEL MDFT TMUX WHICH IS BASED ON THE PROTOTYPE FILTER

coefficients	$g = 3$	$g = 4$	$g = 5$	$g = 6$	$g = 7$	$g = 8$
k_0	+1.00000000	+1.00000000	+1.00000000	+1.00000000	+1.00000000	+1.00000000
k_1	-0.91143783	-0.97195983	-0.99184131	-0.99818572	-0.99938080	-0.99932588
k_2	+0.41143783	+0.70710678	+0.86541624	+0.94838678	+0.97838560	+0.98203168
k_3		-0.23514695	-0.50105361	-0.70710678	-0.84390076	-0.89425129
k_4			+0.12747868	+0.31711593	+0.53649931	+0.70710678
k_5				-0.06021021	-0.20678881	-0.44756522
k_6					+0.03518546	+0.18871614
k_7						-0.03671221
MSA (dB)	32.58	39.86	48.25	58.12	63.45	61.54
ARF	$\|\omega\|^{-3}$	$\|\omega\|^{-3}$	$\|\omega\|^{-5}$	$\|\omega\|^{-5}$	$\|\omega\|^{-7}$	$\|\omega\|^{-7}$
SNR (dB)	49.21	68.31	69.88	89.34	90.09	104.58

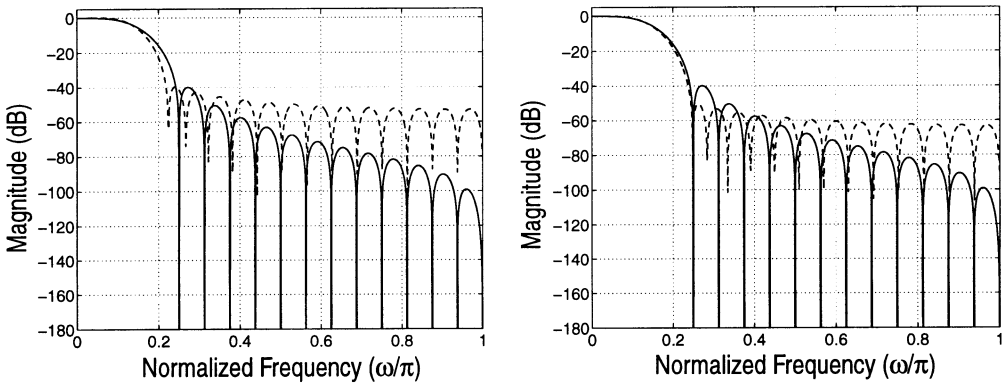

(a) (b)

Fig. 9. Magnitude frequency response of a prototype filter of length 32 designed using the approach proposed in [22]. (a) With the same minimum stopband attenuation. (b) The same transition bandwidth (dashed lines) as that of the proposed prototype filter of length 32 with $g = 4$ (solid lines).

For the purpose of this comparison, two prototype filters of length 32, which are intended for an 8-channel complex-modulated TMUX, are designed based on the technique proposed in [22]. These prototype filters are designed to have the same -3 dB bandwidth as that of our proposed prototype filter of the same length (i.e., length 32 with $g = 4$).

Shown in Fig. 9, are magnitude frequency responses of these two prototype filters (dashed lines). One of the filters is designed to have the same minimum stopband attenuation (maximum sidelobe magnitude) as that of our proposed prototype filter [Fig. 9(a)]. The second one is designed to have a transition band matched to that of the proposed filter [Fig. 9(b)].

From the plots shown in Fig. 9, in both cases, the faster stopband fall-off rate of the proposed filter is evident. Note that in Fig. 9(a) the filter designed using the approach of [22] has a narrower transition bandwidth; however, this should not affect the performance of the TMUX system, because the adjacent channel crosstalks are exactly cancelled. In Fig. 9(b), the filter designed based on the approach of [22] has a better MSA compared to that of the proposed prototype filter; however, it has a slower stopband fall-off rate. For further comparison, Fig. 10 shows the plots of the normalized magnitude of the linear distortion function and the crosstalk distortion function for the TMUX system based on the above prototype filters designed using the approach of [22]. By comparing the plots shown in this figure with the corresponding plots in Fig. 7 and Fig. 8 (i.e., for $g = 4$), the significantly better overall performance of the systems based on the proposed prototype filter is evident.

Next, we compare the proposed prototype filter with a standard root-raised cosine prototype filter [10], [11]. For the purpose of this comparison, two root-raised cosine filters of lengths 33 and 65 with a roll-off factor of 0.75 which are intended for an 8-channel complex-modulated TMUX, are considered. Magnitude frequency responses of these filters along with that of the prototype filter of length 32 (with $g = 4$), and length 64 (with $g = 8$) are shown in Fig. 11. From the plots shown in this figure, the superior stopband performance and frequency containment of the proposed filters are evident. For further comparison of the systems, Fig. 12 shows the plots of the normalized magnitude of the linear distortion function and the crosstalk distortion function for the TMUX system based on the aforementioned root-raised cosine filters. By comparing the plots shown in this figure with the corresponding plots in Figs . 7 and Fig. 8 for the respective proposed prototype filters (i.e., for $g = 4$ and $g = 8$) the much better performance of the systems based on the proposed prototype filters is clear.

As another example, the spectra of the proposed prototype filter and that of [6] (with $g = 8$ and $N = 64$) for an 8-channel

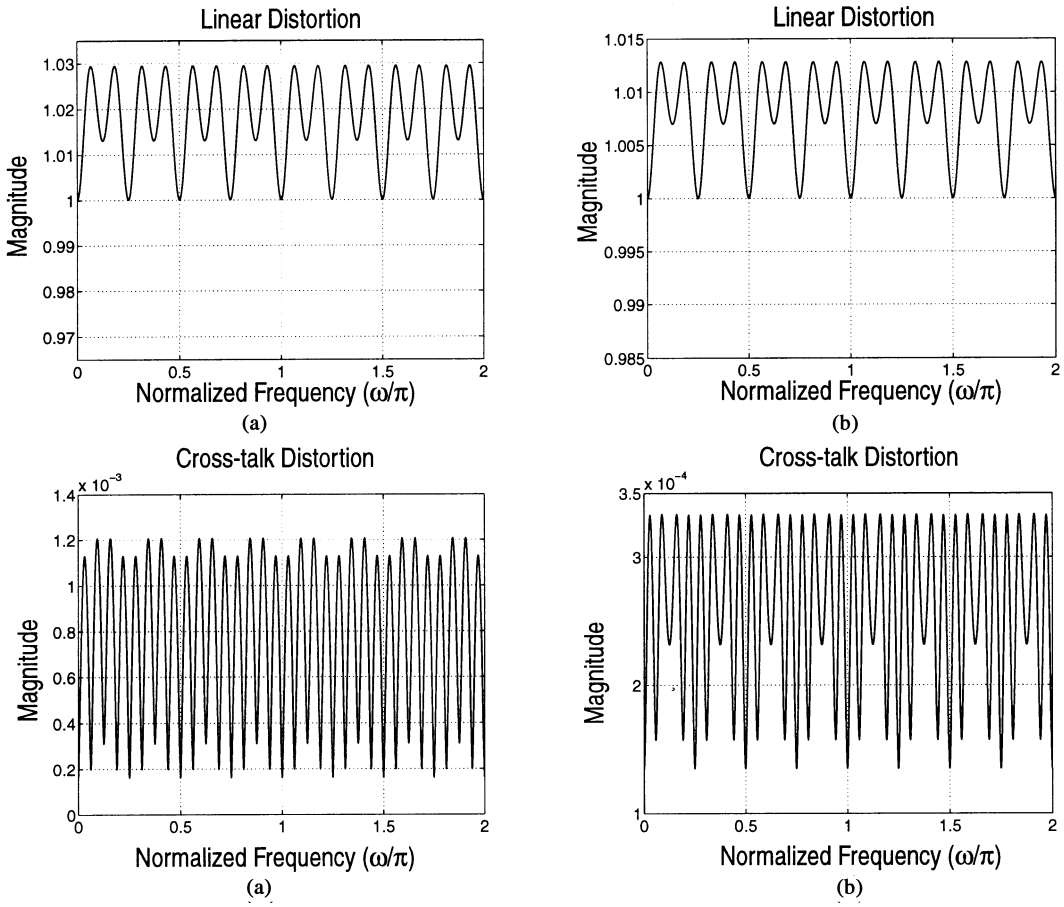

Fig. 10. Normalized magnitude of the linear distortion function for an 8-channel TMUX constructed with a prototype filter of length 32 (designed using the approach proposed in [22]) with the same MSA. (a) The same transition bandwidth as that of the proposed prototype filter, (b) along with the magnitude of the crosstalk distortion function, and (c) (d) for the corresponding TMUXs.

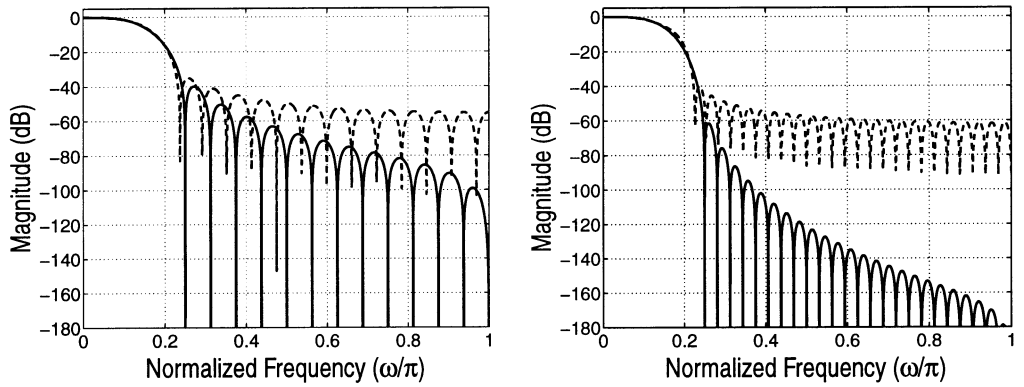

Fig. 11. Magnitude frequency response of a root-raised cosine filter of length (a) 33, and (b) length 65 (dashed lines) along with that of the prototype filter of length (a) 32 with $g = 4$, and (b) length 64 with $g = 8$ (solid lines).

MDFT TMUX are shown in Fig. 13. Also shown in the figure is the line with a fall-off rate proportional to $|\omega|^{-7}$. As expected, the fall-off rate of the proposed filter for large frequencies is faster than $|\omega|^{-7}$. Also, as can be seen from the figure, the fall-off rate of the proposed filter is faster than that of the same order filter of [6], although its first few sidelobes are higher. This result is typical for other values of g. It should be noted that the fall-off rate of the filters proposed in [6] was shown to be superior to that of other filters, such as those in [7].

As a final example, we examine a PR 8-channel filter bank designed based on generalized linear-phase lapped orthogonal transform (GenLOT) [23]. As discussed earlier, in many practical applications, especially data communication applications having interferers, it is often judicious to relax the PR condition by allowing small amplitude and crosstalk (aliasing) distortion, and at the same time achieving the better stopband performance of subchannel filters [1], [6]. The following example will further illustrate this point. For the purpose of this comparison, the

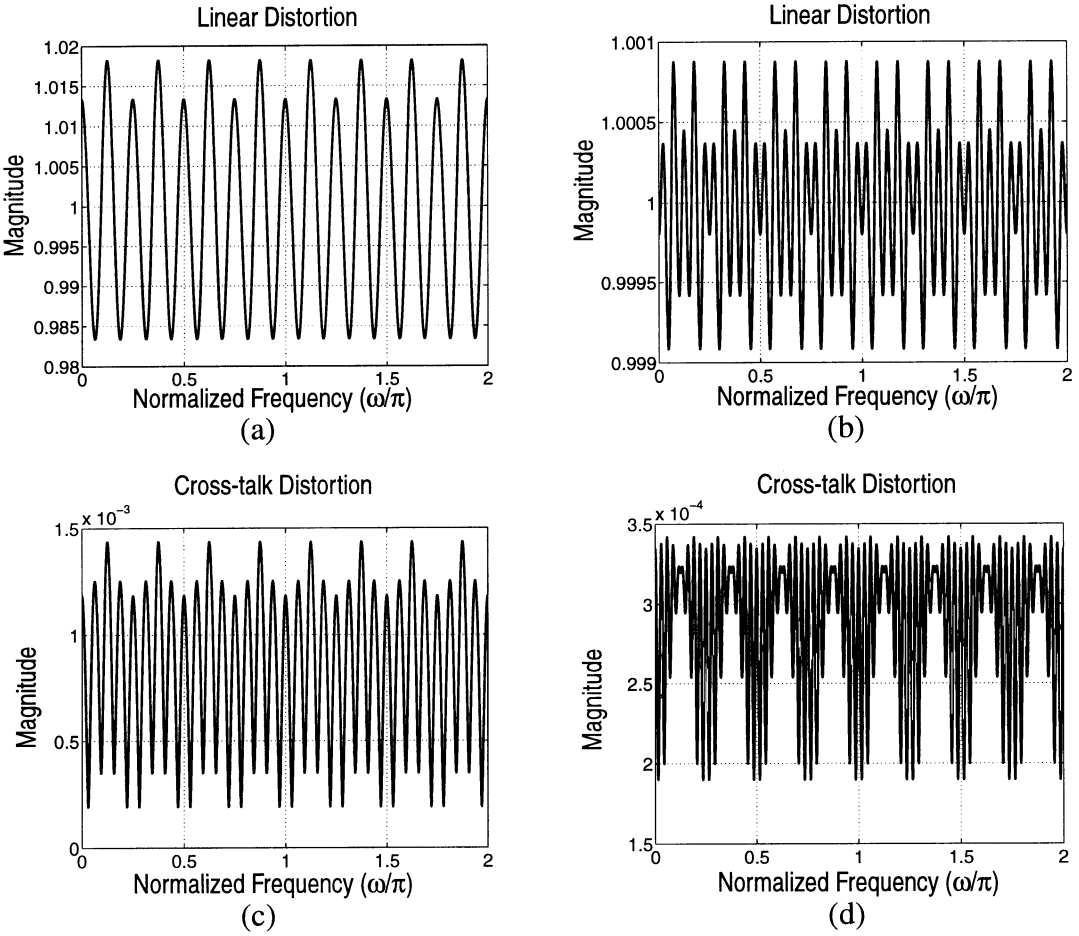

Fig. 12. Normalized magnitude of the linear distortion function for an 8-channel TMUX constructed with a root-raised cosine prototype filter of length (a) 33 and (b) 65 along with the magnitude of the crosstalk distortion function for the corresponding TMUXs.

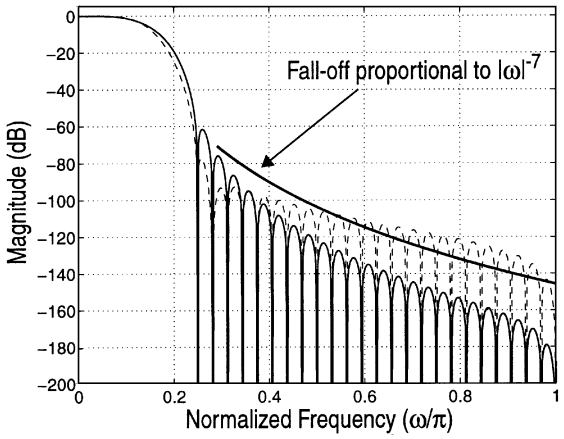

Fig. 13. Spectra of the proposed prototype filter (solid-line) and that of [6] (dashed-line) for $g = 8$ and $N = 64$.

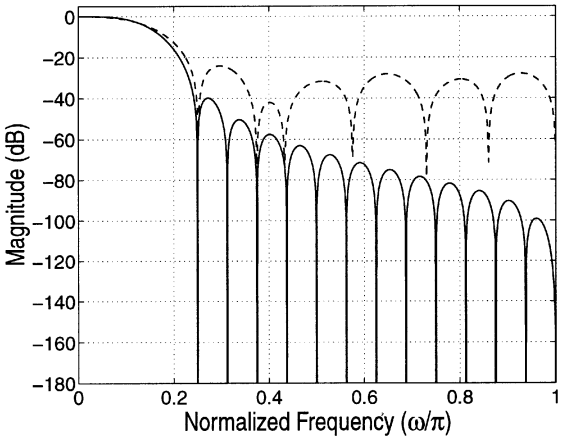

Fig. 14. Spectra of the proposed prototype filter with $g = 4$ and $N = 32$ (solid-line) and that of low-pass filter of an 8-channel GenLOT system with filters of length 32 optimized for maximum stop- band attenuation designed in [23] (dashed-line).

low-pass filter of an 8-channel GenLOT filter bank is considered. The filters of this GenLOT system are optimized for the best stopband attenuation achievable with filters of length 32 [23]. The magnitude frequency response of this low-pass filter and that of the same length proposed prototype filter are shown in Fig. 14. As can be seen from the figure, the fall-off rate of the proposed filter is much faster than that of the same order low-pass filter of the aforementioned 8-channel GenLOT system. Furthermore, the proposed prototype filter has a better stopband attenuation. This result is typical for other values of g.

V. Conclusion

A simple procedure for the design of a highly selective prototype filter for overlapped complex-modulated NPR TMUXs

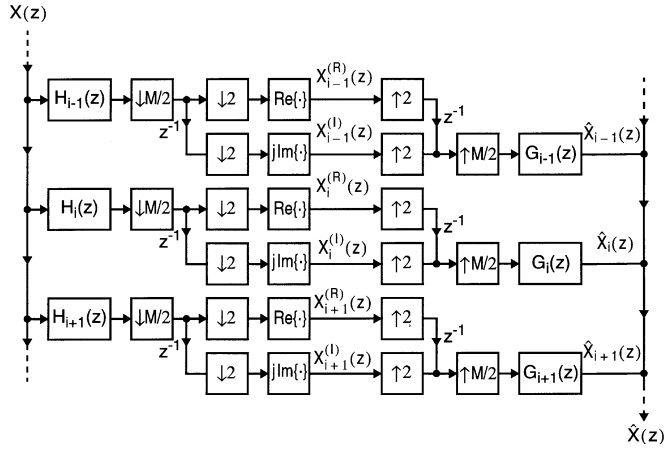

Fig. 15. A Filter bank (dual of the TMUX in Fig. 2).

has been presented. The design method is unified for all values of the overlap factor. The minimum stopband attenuation and the minimum fall-off rate of the sidelobes of the filter has been found to be a function of the overlap factor and independent of the filter order. The fast sidelobe fall-off rate of the designed filter is justified analytically and is superior to that of previously reported linear-phase FIR prototype filters for filter-bank applications.

Appendix A

The structurally-inherent crosstalk cancellation property of the MDFT TMUX of Fig. 1, in which synthesis and analysis filters are constructed from a linear-phase prototype filter using (1) and (2) has been shown in [9], [11], and [12]. In this appendix, we show that the transmultiplexer of Fig. 2, in which the synthesis and analysis filters are constructed from a linear-phase prototype filter using (3) and (4), has also the structurally-inherent crosstalk cancellation property.

Due to the duality between maximally-decimated filter banks and transmultiplexers [8], [11], [13], and since it is easier to show the validity of this property for filter banks (as it has been done in [9] and [12]), we will prove it for filter banks. Note that, in the context of filter banks, the dual (equivalent) of crosstalk is aliasing.

The dual of the M-channel TMUX in Fig. 2 is the M-channel filter bank of Fig. 15. From (3) and (4) we have

$$g_i(n) = j^i \cdot p(n) \cdot W_M^{-in} \tag{A1}$$

$$h_i(n) = g_i{}^*(N-n) \tag{A2}$$

$$= \left[j^i \cdot p(N-n) \cdot W_M^{-i(N-n)} \right]^* \tag{A3}$$

$$= (-1)^i g_i(n) \tag{A4}$$

where W_M is the Mth root of unity defined as $W_M = e^{-j(2\pi/M)}$. Note that for the prototype filter we have: $p(n) = p(N-n)$.

Using (A1) to (A4), it can be shown that

$$h_i{}^*(n) = (-1)^{\frac{M}{2}} h_{M-i}(n). \tag{A5}$$

Then, following the proof procedures of [9] and [12], it can be shown that the z-transform of the output of the filter bank, i.e., $\hat{X}(z)$ can be written as

$$\hat{X}(z) = \frac{z^{\frac{-M}{2}}}{M} \cdot \left\{ \sum_{i=0}^{M-1} G_i(z) \cdot \sum_{k=0}^{\frac{M}{2}-1} H_i\left(zW_M^{2k}\right) X\left(zW_M^{2k}\right) + (-1)^{\frac{M}{2}} \sum_{i=0}^{M-1} G_i(z) \cdot \sum_{k=0}^{\frac{M}{2}-1} H_{M-i}\left(zW_M^{2k+1}\right) \overline{X}\left(zW_M^{2k+1}\right) \right\} \tag{A6}$$

where $\overline{X}(z)$ denotes the z-transform of the complex-conjugate of the input signal, i.e., $x^*(n)$.

We now show that, for $z = e^{j\omega}$ (i.e., in the frequency domain), the second expression in (A6) is identically zero for all values of ω. To prove this, we first express the transfer functions of the analysis and the synthesis filters in terms of the transfer function of the prototype filter. From (A1) and (A2), we have

$$G_i(z) = j^i P\left(zW_M^i\right) \tag{A7}$$

$$H_i(z) = z^{-N} G_i{}^*\left(\frac{1}{z^*}\right) = z^{-N}(-j)^i P^*\left(\frac{1}{z^*} W_M^i\right). \tag{A8}$$

Hence, following the procedure similar to that outlined in [9], [12] (omitting intermediate steps for the sake of brevity), we can write (note that M is an even number)

$$\begin{aligned}
&(-1)^{\frac{M}{2}} \sum_{i=0}^{M-1} G_i(z) \cdot \sum_{k=0}^{\frac{M}{2}-1} H_{M-i}\left(zW_M^{2k+1}\right) \overline{X}\left(zW_M^{2k+1}\right) \\
&= (-1)^{\frac{M}{2}} \sum_{i=0}^{M-1} j^i \cdot P\left(zW_M^i\right) \cdot \sum_{k=0}^{\frac{M}{2}-1} z^{-N} \\
&\quad \cdot (-j)^{M-i} P^*\left(\frac{1}{z^*} W_M^{M-i+2k+1}\right) \overline{X}\left(zW_M^{2k+1}\right) \\
&= z^{-N} \sum_{k=0}^{\frac{M}{2}-1} \overline{X}\left(zW_M^{2k+1}\right) \cdot \left\{ \sum_{i=0}^{\frac{M}{2}-1} P\left(zW_M^{2i}\right) P^*\left(\frac{1}{z^*} W_M^{-2i+2k+1}\right) \right. \\
&\quad \left. - \sum_{i=0}^{\frac{M}{2}-1} P\left(zW_M^{-2i+2k+1}\right) P^*\left(\frac{1}{z^*} W_M^{2i}\right) \right\}.
\end{aligned} \tag{A9}$$

By replacing z with $e^{j\omega}$, we can write the right-hand side (RHS) of (A9) in the frequency domain as

$$e^{-jN\omega} \cdot \sum_{k=0}^{\frac{M}{2}-1} \overline{X}\left(e^{j\omega} W_M^{2k+1}\right) \cdot \sum_{i=0}^{\frac{M}{2}-1} 2j \cdot \mathrm{Im}\left\{ P\left(e^{j\left(\omega - \frac{2\pi(2i)}{M}\right)}\right) \times P^*\left(e^{j\left(\omega - \frac{2\pi(-2i+2k+1)}{M}\right)}\right) \right\}. \tag{A10}$$

Since the prototype filter $p(n)$ is linear-phase, its Fourier transform has the following general form

$$P(e^{j\omega}) = e^{-j\alpha\omega} \cdot K(\omega). \tag{A11}$$

In (A11), α is in general a rational number, and $K(\omega)$ is a real function of ω, i.e., $\mathrm{Im}\{K(\omega)\} = 0$ for all ω. For the prototype filter considered in this work, $\alpha = N/2$ and $K(\omega) = W(e^{j\omega})$. It can be shown that $W(e^{j\omega})$ is a real function of ω. Let us for notational simplicity denote $P(e^{j\omega}) = e^{-jN\omega/2} \cdot K(\omega)$. Then, we have $P^*(e^{j\omega}) = e^{jN\omega/2} \cdot K(\omega)$, and we can write

$$\begin{aligned} & P\left(e^{j\left(\omega-\frac{2\pi(2i)}{M}\right)}\right) P^*\left(e^{j\left(\omega-\frac{2\pi(-2i+2k+1)}{M}\right)}\right) \\ &= e^{-j\frac{N}{2}\left(\frac{2\pi(4i-2k-1)}{M}\right)} \cdot K\left(\omega-\frac{2\pi(2i)}{M}\right) \\ &\quad \times K\left(\omega-\frac{2\pi(-2i+2k+1)}{M}\right) \qquad \text{(A12)} \\ &= e^{jg\pi(4i-2k-1)} \cdot K\left(\omega-\frac{2\pi(2i)}{M}\right) \\ &\quad \times K\left(\omega-\frac{2\pi(-2i+2k+1)}{M}\right). \qquad \text{(A13)} \end{aligned}$$

From (A12) to (A13), we have taken into account that $N = gM$. Since $K(\omega)$ is a real function for all values of ω, the imaginary part of the RHS of (A13) can be written as

$$\begin{aligned} & \mathrm{Im}\left\{e^{jg\pi(4i-2k-1)} \cdot K\left(\omega-\frac{2\pi(2i)}{M}\right) K\left(\omega-\frac{2\pi(-2i+2k+1)}{M}\right)\right\} \\ &= \sin\{g\pi(4i-2k-1)\} \\ &= 0. \end{aligned} \qquad \text{(A14)}$$

That is

$$\mathrm{Im}\left\{P\left(e^{j\left(\omega-\frac{2\pi(2i)}{M}\right)}\right) P^*\left(e^{j\left(\omega-\frac{2\pi(-2i+2k+1)}{M}\right)}\right)\right\} = 0. \qquad \text{(A15)}$$

Thus, from (A6), we can write the output of the filter bank (in the frequency domain) as

$$\hat{X}(e^{j\omega}) = \frac{e^{-\frac{jM\omega}{2}}}{M} \cdot \sum_{i=0}^{M-1} G_i(e^{j\omega}) \cdot \sum_{k=0}^{\frac{M}{2}-1} H_i\left(e^{j\omega} W_M^{2k}\right) X\left(e^{j\omega} W_M^{2k}\right). \qquad \text{(A16)}$$

From (A16), it can be seen that all odd aliasing terms of $\hat{X}(e^{j\omega})$ are cancelled. Using the duality between the filter bank of Fig. 15 and the transmultiplexer of Fig. 2, this alias-cancellation property implies that, in the transmultiplexer, the crosstalk between any two channels with an odd-numbered difference between their indices is cancelled.

Notice that, if the prototype filter has a sufficiently high stopband attenuation and a fast fall-off rate, then

$$G_i(e^{j\omega}) \cdot H_i\left(e^{j\omega} W_M^{2k}\right) \approx 0 \quad \text{for } k = 1, 2, \ldots, \frac{M}{2} - 1. \qquad \text{(A17)}$$

In this case, we can rewrite (A16) as

$$\hat{X}(e^{j\omega}) \approx \frac{e^{-\frac{jM\omega}{2}}}{M} \cdot \sum_{i=0}^{M-1} G_i(e^{j\omega}) \cdot H_i(e^{j\omega}) X(e^{j\omega}). \qquad \text{(A18)}$$

Therefore, we have

$$T(e^{j\omega}) = \frac{\hat{X}(e^{j\omega})}{X(e^{j\omega})} \approx \frac{e^{-\frac{jM\omega}{2}}}{M} \cdot \sum_{i=0}^{M-1} G_i(e^{j\omega}) \cdot H_i(e^{j\omega}). \qquad \text{(A19)}$$

In order to have a (near) perfect reconstruction filter bank, the transfer function in (A19) should be equivalent to a pure delay with possibly a nonzero gain [8], [11], i.e.,

$$T(e^{j\omega}) = \gamma \cdot e^{-j\omega n_0}. \qquad \text{(A20)}$$

Note, that in general γ is a complex number. Considering (A.19) and (A20), the overall filter bank system has a (near) perfect-reconstruction property if the following condition (approximately) holds

$$\left| \sum_{i=0}^{M-1} G_i(e^{j\omega}) H_i(e^{j\omega}) \right| = c \qquad \text{(A21)}$$

where $c = M \cdot |\gamma|$ Again, due to the duality, the transmultiplexer of Fig. 2 has a (near) perfect-reconstruction property, if (A21) (approximately) holds.

As a final point, note that as discussed in [8], [11], and [12], the following distortion function can be considered as a measure of aliasing distortion in the filter bank of Fig. 15. Equivalently, due to the duality it can be used as a measure of crosstalk distortion in the TMUX of Fig. 2

$$D(e^{j\omega}) = \left(\sum_{k=1}^{M-1} \frac{1}{M} \left| \sum_{i=0}^{M-1} G_i(e^{j\omega}) \cdot H_i\left(e^{j\omega} W_M^k\right) \right|^2 \right)^{\frac{1}{2}}. \qquad \text{(A22)}$$

REFERENCES

[1] A. Viholainen, T. Saramäki, and M. Renfors, "Nearly perfect-reconstruction cosine-modulated filter bank design for VDSL modems," in *Proc. IEEE 6th Int. Conf. Electronics, Circuits, and Systems*, vol. 1, Sept. 1999, pp. 373–376.

[2] A. N. Akunsu, P. Duhamel, X. Lin, and M. de Courville, "Orthogonal transmultiplexers in communications: a review," *IEEE Trans. Signal Processing*, vol. 46, pp. 979–995, Apr. 1998.

[3] P. P. Vaidyanathan, "Filter banks in digital communications," *IEEE Circuits Syst. Mag.*, vol. 1, pp. 4–25, 2001.

[4] S. Govardhanagiri, T. Karp, P. Heller, and T. Nguyen, "Performance analysis of multicarrier modulation systems using cosine modulated filter banks," in *Proc. IEEE Int. Conf. Acoustics, Speech and Signal Processing, ICASSP-1999*, vol. 3, pp. 1405–1408.

[5] T. Ihalainen, J. Alhava, A. Viholainen, H. Xing, J. Rinne, and M. Renfors, "On the performance of filter bank based multicarrier systems in XDSL and WLAN applications," in *Proc. IEEE Int. Conf. Communications, ICC-2000*, vol. 2, pp. 1120–1124.

[6] K. W. Martin, "Small sidelobe filter design for multitone data-communication applications," *IEEE Trans. Circuits Syst. II*, vol. 45, pp. 1155–1161, Aug. 1998.

[7] S. D. Sandberg and M. A. Tzannes, "Overlapped discrete multitone modulation for high speed copper wire communications," *IEEE J. Select. Area Commun.*, vol. 13, pp. 1571–1585, Dec. 1995.

[8] P. P. Vaidyanathan, *Multirate Systems and Filter Banks*. Englewood Cliffs, NJ: Prentice-Hall, 1993.

[9] P. N. Heller, T. Karp, and T. Q. Nguyen, "A general formulation of modulated filter banks," *IEEE Trans. Signal Processing*, vol. 47, pp. 986–1002, Apr. 1999.

[10] G. Rösel and N. J. Fliege, "Transmultiplexer filter banks with extremely low crosstalk and intersymbol interference," in *Proc. IEEE Int. Symp.. Circuits and Systems, ISCAS-1995*, vol. 2, pp. 1448–1451.

[11] N. J. Fliege, *Multirate Digital Signal Processing*. New York: Wiley, 1999.

[12] T. Karp and N. J. Fliege, "Modified DFT filter banks with perfect reconstruction," *IEEE Transa. Circuits Syst. II*, vol. 46, pp. 1404–1414, Nov. 1999.

[13] M. Vetterli, "Perfect transmultiplexers," in *Proc. IEEE Int. Conf. Acoustics, Speech and Signal Processing, ICASSP-1986*, vol. 4, 1986, pp. 2567–2570.

[14] F. J. Harris, "On the use of windows for harmonic analysis with the discrete fourier transform," *Proc. IEEE*, vol. 66, pp. 51–83, Jan. 1978.
[15] A. H. Nuttall, "Some windows with very good sidelobe behavior," *IEEE Trans. Acoust., Speech, Signal Processing*, vol. 29, pp. 84–91, Feb. 1981.
[16] J. Zhong, Z. Han, and W. Lu, "Design of windows with steerable sidelobe dips," *IEEE Trans. Signal Processing*, vol. 40, pp. 1452–1459, June 1992.
[17] M. T. Hanna, "Windows with rapidly decaying sidelobes and steerable sidelobe dips," *IEEE Trans. Signal Processing*, vol. 42, pp. 2037–2044, Aug. 1994.
[18] R. N. Bracewell, *The Fourier Transform and Its Applications*. New York: McGraw-Hill, 2000.
[19] A. Papoulis, *Signal Analysis*. New York: McGraw-Hill, 1977.
[20] A. V. Oppenheim, R. W. Schafer, and J. R. Buck, *Discrete-Time Signal Processing*. Englewood Cliffs, NJ: Prentice-Hall, 1999.
[21] L. R. Rabiner and B. Gold, *Theory and Application of Digital Signal Processing*. Englewood Cliffs, NJ: Prentice-Hall, 1975.
[22] Y. Lin and P. P. Vaidyanathan, "A Kaiser window approach for the design of prototype filters of cosine modulated filterbanks," *IEEE Signal Processing Lett.*, vol. 5, pp. 132–134, June 1998.
[23] R. L. de Queiroz, T. N. Nguyen, and K. R. Rao, "The GenLOT: Generalized Linear-Phase Lapped Orthogonal Transform," *IEEE Trans. Signal Processing*, vol. 44, pp. 497–507, Mar. 1996.

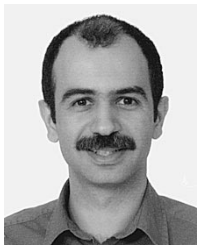

Shahriar Mirabbasi (S'95–M'03) received the B.Sc. degree in electrical engineering from Sharif University of Technology, Tehran, Iran, in 1990 and the M.A.Sc. and Ph.D. degrees in electrical and computer engineering from the University of Toronto, ON, Canada, in 1997 and 2002, respectively.

In summer 1997, he was with Gennum Corporation, Burlington, ON, Canada, working on the design of cable equalizers for serial digital video and HDTV applications. From 2001 to 2002, he was with Snowbush Microelectronics, Toronto, ON, Canada, as a Designer where he worked on high-speed mixed-signal CMOS integrated circuits including ADC and serializer/deserializer blocks. Since 2002, he has been an Assistant Professor in the Department of Electrical and Computer Engineering, University of British Columbia, Vancouver, BC, Canada. His current research interests include analog and mixed-signal integrated circuits and systems design for high-speed data communications applications, low-power integrated transceiver design, and multirate signal processing.

Kenneth W. Martin (S'75–M'80–SM'89–F'91) received the B.A.Sc., M.A.Sc., and Ph.D. degrees from the University of Toronto, ON, Canada, in 1975, 1977, and 1980, respectively.

From 1977 to 1978, he was a Member of the Scientific Research Staff, Bell Northern Research, Ottawa, ON, Canada, where he worked in the early research on integrated, switched-capacitor networks. Between 1980 and 1992, he was consecutively an Assistant, Associate, and Full Professor at the University of California Los Angeles. In 1992, he accepted the endowed *Stanley Ho Professorship in Microelectronics* at the University of Toronto. In 1998, he cofounded Snowbush Microelectronics and is currently President. He has authored or co-authored two textbooks entitled *Analog Integrated Circuit Design* (New York: Wiley, 1997) and *Digital Integrated Circuit Design* (New York: Oxford, 2000). He has also coauthored three research books with former doctoral Students. He has published over 100 papers and has five patents.

Dr. Martin served as Press Representative for IEEE Circuits and Systems from 1985 to 1986. In 1984, he received the Outstanding Young Engineer Award, by the Circuits and Systems Society, presented at the*IEEE Centennial Keys to the Future Program*. He was elected by the Circuits and Systems Society to their administrative committee (ADCOM) from 1985 to 1987, and as a Member of the *Circuits and Systems BOG* from 1995 to 1997. He served as an Associate Editor of the IEEE TRANSACTIONS ON CIRCUITS AND SYSTEMS from 1985 to 1987, and as an Associate Editor of *Proceedings of the IEEE* from 1995 to 1997. He has also served on the technical committee for many International Symposia on Circuits and Systems and on the Analog Program Committee of the International Solid-State Circuits Committee. He was awarded National Science Foundation Presidential Young Investigator from 1985 to 1990. In 1993, he was a corecipient of the Beatrice Winner Award at the International Solid-State Circuits Conference, and a corecipient of the 1999 IEEE Darlington Best Paper Award for IEEE TRANSACTIONS ON CIRCUITS AND SYSTEMS. In 1999, he received the CAS Golden Jubilee Medal of the IEEE Circuits and Systems Society.